



## Heat transfer enhancement using nanofluids in an automotive cooling system <sup>☆</sup>



Adnan M. Hussein <sup>a,b,\*</sup>, R.A. Bakar <sup>a</sup>, K. Kadirgama <sup>a</sup>, K.V. Sharma <sup>c</sup>

<sup>a</sup> Faculty of Mechanical Engineering, University Malaysia Pahang, 26600 Pekan, Pahang, Malaysia

<sup>b</sup> Al-Haweeja Institute, Foundation of Technical Education, Iraq

<sup>c</sup> Department of Mechanical Engineering, JNTUH College of Engineering, Manthani, India

### ARTICLE INFO

Available online 5 February 2014

#### Keywords:

Laminar  
Nanofluid  
Heat transfer  
Car radiator  
Statistical analysis

### ABSTRACT

The increasing demand of nanofluids in industrial applications has led to increased attention from many researchers. In this paper, heat transfer enhancement using TiO<sub>2</sub> and SiO<sub>2</sub> nanopowders suspended in pure water is presented. The test setup includes a car radiator, and the effects on heat transfer enhancement under the operating conditions are analyzed under laminar flow conditions. The volume flow rate, inlet temperature and nanofluid volume concentration are in the range of 2–8 LPM, 60–80 °C and 1–2% respectively. The results showed that the Nusselt number increased with volume flow rate and slightly increased with inlet temperature and nanofluid volume concentration. The regression equation for input (volume flow rate, inlet temperature and nanofluid volume concentration) and response (Nusselt number) was found. The results of the analysis indicated that significant input parameters to enhance heat transfer with car radiator. These experimental results were found to be in good agreement with other researchers' data, with a deviation of only approximately 4%.

© 2014 Elsevier Ltd. All rights reserved.

### 1. Introduction

The main reason solid particles less than 100 nm are added to a liquid is to improve its thermal properties; this new fluid is then defined as a nanofluid. Solid metallic or nonmetallic materials dispersed in base fluids such as water, ethylene glycol and glycerol have become a topic of interest in recent years [1–7]. There are various applications of thermo fluid systems, including automotive cooling systems [8,9]. Base fluids (water, ethylene glycol and glycerol) have been used as conventional coolants in an automobile radiator for many years; however, these offered low thermal conductivity, which has prompted researchers to find fluids that offer higher thermal conductivity compared to that of conventional coolants. This resulted in nanofluids being used instead of these base fluids [10,11]. Forced convection heat transfer to cool circulating water from an automobile radiator was carried out by Peyghambarzadeh et al. [12]. The effects of different amounts of Al<sub>2</sub>O<sub>3</sub> nanoparticles on the heat transfer performance of the automobile radiator were determined experimentally. The range of flowrate changed from 2 to 6 LPM with the changing inlet temperature of the fluid for all the experiments. The results showed a 40% increase in heat transfer by nanofluids compared to water. A numerical study of laminar heat transfer (CuO and Al<sub>2</sub>O<sub>3</sub>) with ethylene glycol and water inside the flat tube of a car radiator was carried out by Vajjha

et al. [13]. A CFD model of the mass flow rate of air passing across the car radiator was introduced by Trivedi and Vasava [14]. The airflow simulation was created using the commercial software ANSYS 12.1 with the geometry defined using SolidWorks software, and this was followed by meshing, which created the surface mesh as well as the volume mesh accordingly. The results were compared and verified according to the known physical situation and existing experimental data. The results obtained serve as a database for future investigations. New correlations for the viscosity and thermal conductivity of nanofluids as a function of particle volumetric concentration and temperature developed from the experiments are used throughout this paper. The convective heat transfer coefficient and shear stress with the nanofluid showed marked improvement over the base fluid and showed higher magnitudes in the flat regions of the tube. The results showed that the increase in the nanofluid volume fractions due to the increase in the friction factors and convective heat transfer coefficient also increased the pressure loss. Numerical analysis of mixed convection flows in a U-shaped groove's tube in a radiator was conducted by Park and Pak [15]. The Modified SIMPLE algorithm for irregular geometry was developed to determine flow and temperature field. The results were used as fundamental data for tube design, suggesting optimal specifications for radiator tubes. Two liquids, water and an ethylene glycol–water mixture, were used as coolant fluid in a meso-channel heat exchanger and were studied numerically by Dehghandokhta et al. [16]. The results of numerical analysis were compared with the experimental data for the same geometrical and operating conditions to predict heat transfer rate, pressure and temperature drops in the coolants, and there was

<sup>☆</sup> Communicated by W.J. Minkowycz

\* Correspondence author.

E-mail address: [adnanphd2012@gmail.com](mailto:adnanphd2012@gmail.com) (A.M. Hussein).

### Nomenclatures

$C$	Specific heat [ $\text{W/kg} \cdot ^\circ\text{C}$ ]
$D$	Diameter [m]
$E$	Energy [W]
$f$	Friction factor
$h_{tc}$	convection heat transfer coefficient [ $\text{W/m}^2 \cdot ^\circ\text{C}$ ]
$k$	Thermal conductivity [ $\text{W/m} \cdot ^\circ\text{C}$ ]
$Nu$	Nusselt Number [ $h_{tc} \cdot D / K_{nf}$ ]
$P$	Pressure [ $\text{N/m}^2$ ]
$Pr$	Prandtl Number [ $C \cdot \mu / K_{nf}$ ]
$Re$	Reynolds Number [ $\rho_{nf} D_h \cdot u / K_{nf}$ ]
$u$	Velocity [m/s]
$\mu$	Viscosity [ $\text{N} \cdot \text{s/m}^2$ ]
$\rho$	Density [ $\text{kg/m}^3$ ]
$\tau$	Shear stress [ $\text{N/m}^2$ ]
$\phi$	Volume concentration

### Subscripts

$f$	liquid phases
$p$	solid particle
$nf$	nanofluid
$h$	hydraulic

good agreement. Additionally, results showed that the heat exchanger enhanced the heat transfer rate by approximately 20% compared to a straight slab of the same length, and the enhanced heat exchanger has a good potential application as a car radiator with reasonably enhanced heat transfer characteristics compared to an ethylene glycol–water mixture as the coolant. The applications of copper–ethylene glycol nanofluids in a car cooling system have been studied by Leong et al. [17].

In this paper, the Nusselt number of  $\text{TiO}_2$  and  $\text{SiO}_2$  nanopowders suspended in water was evaluated experimentally. The test rig setup included the car radiator and the effects on heat transfer enhancement during operation were analyzed under laminar flow conditions. It should be noted that few studies have reported experimental data on the use of  $\text{TiO}_2$  and  $\text{SiO}_2$  nanofluid in an automotive cooling system. Furthermore, the effects of volume flow rate, inlet temperature and nanofluid volume concentration on the Nusselt number for the car radiator were studied. The regression equations for input (volume flow rate, inlet temperature and nanofluid volume concentration) and output (Nusselt number) parameters were found.

## 2. Experimental work

### 2.1. Experimental setup and procedure

The test rig shown in Fig. 1a was used to measure the heat transfer coefficient in the automotive radiator. This experimental setup includes

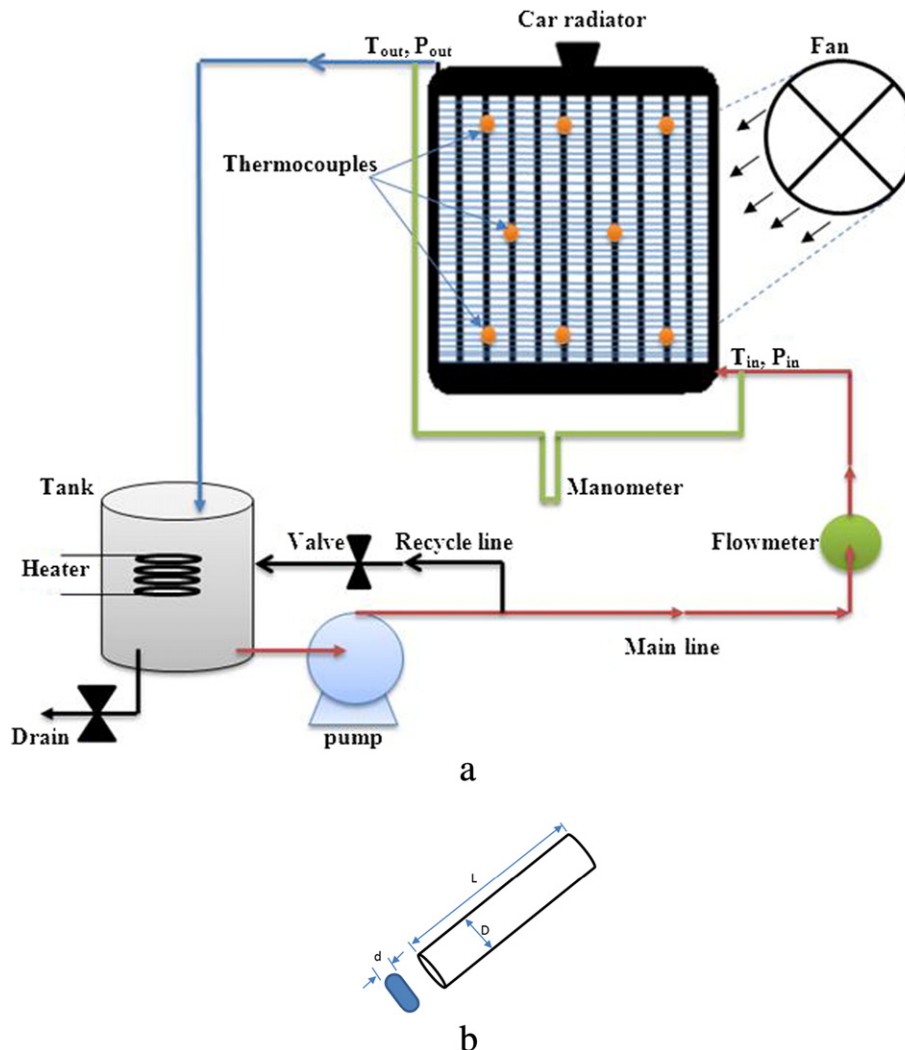


Fig. 1. a—Schematic diagram of the experimental setup, and b—Flat tube of the radiator.

a plastic reservoir tank, an electric heater, a centrifugal pump, a flowmeter, tubes, valves, a fan, a DC power supply, ten T-type thermocouples for temperature measurement, and a heat exchanger (automobile radiator). An electric heater (1500 W) inside a plastic storage tank (40 cm height and 30 cm diameter) was used to represent the engine and to heat the fluid. A voltage regulator (0–220 V) provided the power to regulate the temperature in the radiator (60–80 °C). A flowmeter (0–70 LPM) and two valves were used to measure and control the flowrate. The fluid flow was measured through plastic tubes (0.5 in.) by a centrifugal pump (0.5 hp and 3 m head) from the tank to the radiator at the flow rate range of 2–8 LPM. The total volume of the circulating fluid (3 l) was constant in all experimental steps. Two T-type thermocouples (copper–constantan) were connected to the flow line to record inlet and outlet temperatures of fluid. Eight T-type thermocouples also connected with the radiator surface for the surface area measurement. Due to the very small thickness and high thermal conductivity of the copper flat tubes, the inner and outer surfaces of the tube are equal temperature. A hand-held (–40 °C to 1000 °C) digital thermometer with the accuracy of ±0.1% was used to read all the temperatures from thermocouples. Calibration of thermocouples and thermometers was carried out using a constant temperature water bath, and their accuracy was estimated to be 0.15 °C Peyghambarzadeh et al. [18]. Two small plastic tubes with a 0.25 inch diameter were connected at the inlet and outlet of the radiator and joined to U-tube mercury manometer with accurately scaled 0.5 mmHg to measure the pressure drop at the inlet and outlet. The car radiator has louvered fins and 32 flat vertical copper tubes with a flat cross-sectional area. The distance between the tube rows was filled with thin perpendicular copper fins. For the air side, an axial force fan (1500 rpm) was installed close on axis line of the radiator. The DC power supply (type Teletron 10–12 V) was used instead of a car battery to turn the axial fan.

2.2. Experimental data collection

According to Newton’s cooling law the following procedure was followed to obtain the heat transfer coefficient and corresponding Nusselt number as [19]:

$$Q = hA\Delta T = hA_s(T_b - T_s) \tag{1}$$

$A_s$  is surface area of tube,  $T_b$  is the bulk temperature:

$$T_b = \frac{T_{in} + T_{out}}{2} \tag{2}$$

( $T_{in}$ ,  $T_{out}$ ) are inlet and outlet temperatures and  $T_s$  is the tube wall temperature which is the mean value measured by the two surface thermocouples as:

$$T_s = \frac{T_1 + \dots + T_8}{8} \tag{3}$$

Heat transfer rate is calculated by:

$$Q = mC\Delta T = \dot{m}C(T_{in} - T_{out}) \tag{4}$$

$\dot{m}$  is the mass flow rate, which is determined as:

$$\dot{m} = \rho \times V \tag{5}$$

The heat transfer coefficient can be evaluated by collecting Eqs. (1) and (4):

$$h_{exp} = \frac{\dot{m}C(T_{in} - T_{out})}{nA_s(T_b - T_s)} \tag{6}$$

**Table 1**  
Thermal properties of nanoparticles and base fluids.

Materials	Density (Kg/m <sup>3</sup> )	Specific heat (J/Kg·°K)	Thermal conductivity (W/m·°K)	Viscosity (Pa·s)	References
Pure water	998	4180	0.6067	0.0014	[20]
TiO <sub>2</sub>	4175	692	8.4	–	[20]
SiO <sub>2</sub>	1009	4110	0.56	–	[23]

where  $n$  is a number of radiator tubes, and the Nusselt number can be calculated as:

$$Nu = \frac{h_{exp} \times D_h}{k} \tag{7}$$

$D_h$  is the hydraulic diameter of the tube which estimated by describing the problem undertaken as cylindrical geometry coordinates showed in Fig. 1b. The dimensions of the flat tube are the major and minor diameters ( $D = 9\text{ mm}$ ,  $d = 3\text{ mm}$ , respectively), the length ( $L$ ; 500 mm) and the hydraulic diameter ( $D_h = 4.68\text{ mm}$ ). The Reynolds number is calculated using the hydraulic diameter ( $D_h$ ) which is calculated as [20]:

$$D_h = \frac{4 \times \left[ \frac{\pi}{4}d^2 + (D-d) \times d \right]}{\pi \times d + 2 \times (D-d)} \tag{8}$$

Assuming all thermal properties are estimated at the bulk temperature of the fluid as in Table 1

Reynolds number ( $Re$ ) is determined as:

$$Re = \frac{\rho \times D_h \times u}{\mu} \tag{9}$$

where  $u$  is the velocity at the inlet of the radiator, which is calculated based on the volumetric flow rate ( $V$ ) and cross sectional area ( $A_c$ ) of the tube as:

$$u = \frac{V}{n \times A_c} \tag{10}$$

3. Results and discussions

A number of experimental runs with pure water were conducted with the cooling system to verify the experimental results. The experimental results for  $Nu$  compared with the equations of Shah-London Eq. (11) at laminar flow [12] were as follows:

$$Nu_{av} = 1.953 \left( Re_{D_h} Pr \frac{D_h}{L} \right)^{\frac{1}{3}} \quad \text{for } (Re Pr D_h/L) \geq 33.33$$

$$Nu_{av} = 4.364 + 0.0722 \left( Re_{D_h} Pr \frac{D_h}{L} \right) \quad \text{for } (Re Pr D_h/L) < 33.33 \tag{11}$$

Fig. 2 shows the experimental data for the Nusselt number with different Reynolds numbers for pure water. It seems that the experimental data for pure water agreed with Shah-London Eq. (11) for laminar flow. The effect of nanoparticle concentration

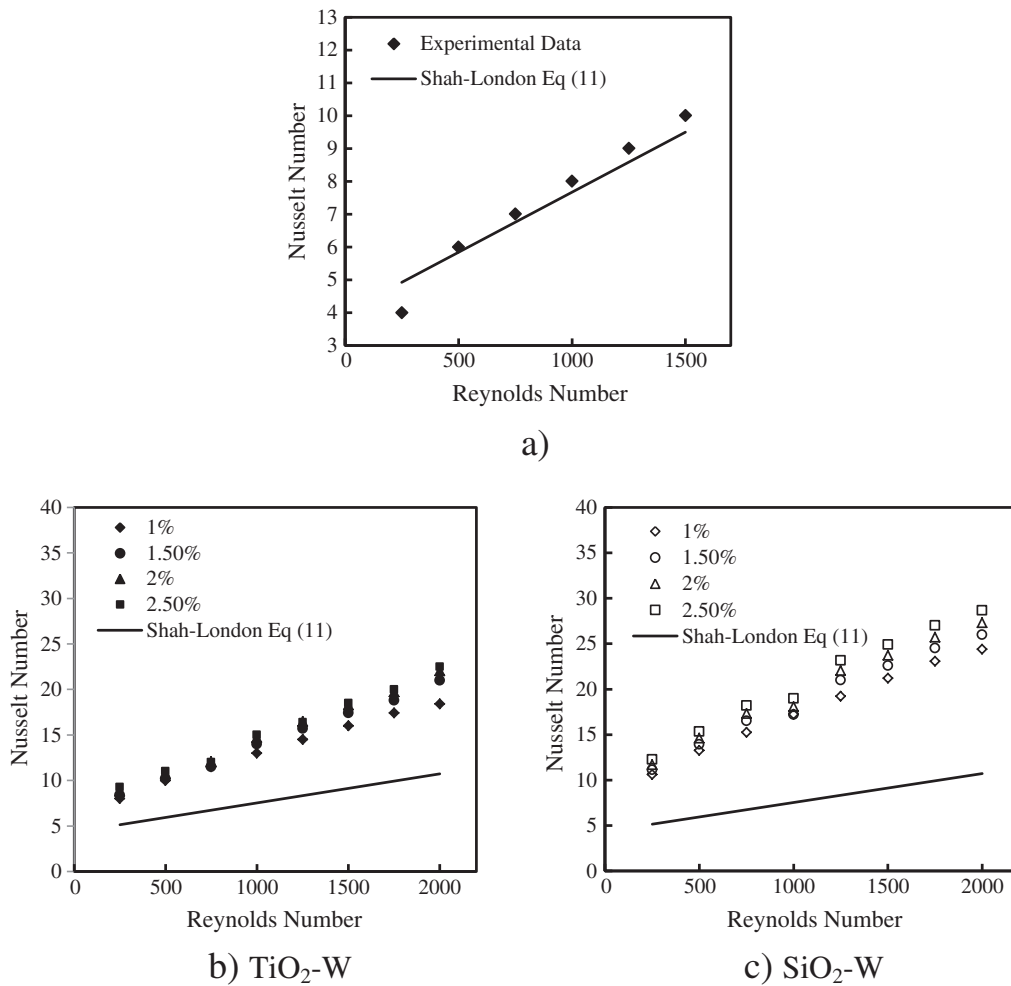


Fig. 2. Nusselt numbers at different Reynolds numbers: a–pure water, b– $\text{TiO}_2\text{-W}$ , and c– $\text{SiO}_2\text{-W}$ .

on the average Nusselt number is indicated in Fig. 3 for  $\text{TiO}_2\text{-W}$  and  $\text{SiO}_2\text{-W}$ , respectively. It seems that the Nusselt number increases with increasing Reynolds number and volume concentration. The maximum values of the Nusselt number are 18.11733 and 20.63152 for  $\text{TiO}_2\text{-W}$  and  $\text{SiO}_2\text{-W}$ , respectively. It appears that a

$\text{SiO}_2\text{-W}$  nanofluid is better than  $\text{TiO}_2\text{-W}$  for heat transfer enhancement, while  $\text{TiO}_2\text{-W}$  was shown to give a significant enhancement of heat transfer compared with pure water. Fig. 3 also included a comparison of the Nusselt number among nanofluids and base fluids at laminar flow. This comparison shows that the nanofluid has higher

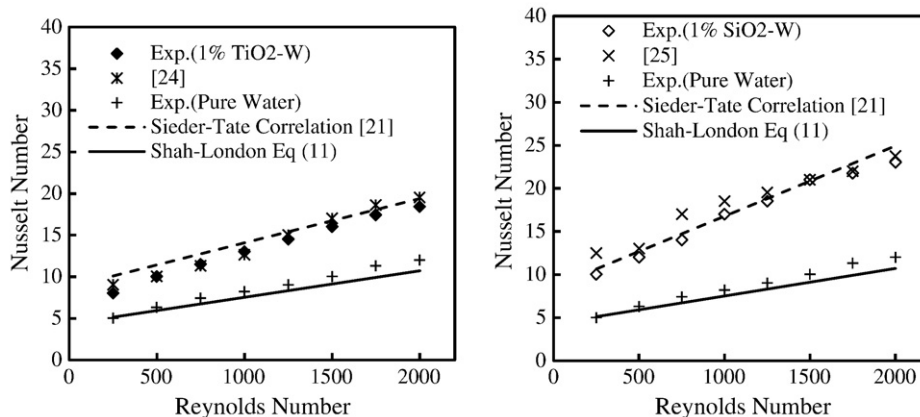


Fig. 3. Validation of the Nusselt number with equations and experimental data: a– $\text{TiO}_2\text{-W}$ , b– $\text{SiO}_2\text{-W}$ .

values of heat transfer enhancement than the base fluid. The other side illustrates the experimental data for the Nusselt number with curve-fitting data of [24,25], Sieder-Tate correlation [21] and Shah-London Eq. (11) for both TiO<sub>2</sub>-W and SiO<sub>2</sub>-W. The maximum enhancement of the Nusselt number is 22.5% when nanofluids and pure water are compared.

3.1. Experimental design and data analysis

In this work, only the significant parameters were used to develop mathematical models using factorial methodology (FM). FM is a collection of mathematical and statistical techniques that are useful for the modeling and analysis of problems in which the response of interest is influenced by several variables and the objective is to optimize the response [26–29]. Variable levels of the parameters used in the experimental analysis are shown in Table 2. Experimental results from the cooling system with pure water and (TiO<sub>2</sub> and SiO<sub>2</sub>) nanofluids are presented and tabulated in Tables 3 and 4. The response parameter is the Nusselt number (Nu) under laminar flow, and the input parameters are volume flow rate (Q), inlet temperature (T) and the volume concentration of the nanofluid according to the full factorial design. The results showed that the minimal values of Nu were obtained at Q = 2 LPM, T = 60 °C and φ = 0.01 (test no. 1), and the maximal values of Nu were found at Q = 8 LPM, T = 80 °C and φ = 0.02 (test no. 27). Nu increased with all three components. Likewise, the values of Nu for SiO<sub>2</sub>-W are higher than for TiO<sub>2</sub>-W, and the last one has values higher than pure water.

3.2. ANOVA for Nu

The results of the analysis of variance (ANOVA) for Nu are shown in Table 5, which includes the degrees of freedom (DF), the sum of squares (SS), mean squares (MS), F-values (F) and probability (P) of each factor and different interactions. A low P-value (≤0.05) indicates statistical significance for the source on the corresponding response (i.e., α = 0.05, or 95% confidence level). This indicates that the obtained models are considered to be statistically significant as it demonstrates that the terms in the model have a significant effect on the response Frides et al. [30]. The other important coefficient (R-Sq), which is called the coefficient of determination in the resulting ANOVA tables, is defined as the ratio of the explained variation to the total variation and is a measure of the fitting degree. As R-Sq approaches unity, a good correlation between the experimental and the predicted values is indicated. It is clear from the results of ANOVA that the heat transfer enhancement is considerable. For pure water, it is noted in Table 5a that Q and T are significant with R-Sq = 96.36% and R-Sq(adj) = 94.18%, but the interaction Q \* T is not significant. The Q, T, φ, Q \* T and Q \* φ are significant for the TiO<sub>2</sub>-W nanofluid as shown in Table 5b with R-Sq = 99.56% and R-Sq(adj) = 99.40%. The Q, T and φ are significant for the SiO<sub>2</sub>-W nanofluid as shown in Table 5c with R-Sq = 92.76% and R-Sq(adj) = 90.10%. The P-value of less than 0.05 indicates the significance of these parameters. It seems that the values of R-Sq are close to R-Sq(adj), so the analysis is accepted. The mathematical model was developed using estimated coefficients for Nu to understand the heat transfer process in terms of volume flow rate, inlet

Table 2 Variable levels.

Level	Q (LPM)	T (°C)	φ
Low	2	60	0.01
Medium	5	70	0.015
High	8	80	0.02

Table 3 Design layout and experimental results for pure water.

Test no.	Q (LPM)	T °C	Nu
1	2	60	5.238034
2	5	60	7.818839
3	8	60	13.51095
4	2	70	5.688422
5	5	70	8.229778
6	8	70	14.22106
7	2	80	5.869919
8	5	80	9.940991
9	8	80	16.16633

temperature and nanofluid volume concentration for the cooling system, as shown in Table 6. However, this model is built using only the parameters with significant interactions. Nu models are given by Eqs. (12), (13) and (14) for pure water, TiO<sub>2</sub>-W and SiO<sub>2</sub>-W, respectively.

$$Nu = 1.69414 + 0.32529 * Q + 0.0058446 * T \tag{12}$$

$$Nu = 6.38776 + 0.06018 * Q - 0.0610291 * T - 285.668 * \phi + 0.0176852 * (Q * T) + 51.2556 * (Q * \phi) \tag{13}$$

$$Nu = -3.0125 - 1.31736 * Q + 0.083777 * T - 1071.89 * \phi \tag{14}$$

3.3. Main effects of parameters on Nu

Fig. 4 shows the main factor plots for Nu of pure water, TiO<sub>2</sub>-W and SiO<sub>2</sub>-W, respectively. The volume flow rate appears to be an

Table 4 Design layout and experimental results for nanofluids.

Test no.	Q (LPM)	T °C	φ	TiO <sub>2</sub> -W	SiO <sub>2</sub> -W
				Nu	Nu
1	2	60	0.01	5.434521	5.752052
2	5	60	0.01	9.474881	10.11103
3	8	60	0.01	14.03381	14.84401
4	2	70	0.01	5.766007	5.935275
5	5	70	0.01	9.82842	10.4183
6	8	70	0.01	14.41502	17.37154
7	2	80	0.01	5.977887	12.42765
8	5	80	0.01	10.09424	13.06611
9	8	80	0.01	16.2865	22.11002
10	2	60	0.015	5.634525	6.08163
11	5	60	0.015	9.949783	11.83651
12	8	60	0.015	15.36689	16.60753
13	2	70	0.015	5.952814	6.310522
14	5	70	0.015	10.89577	12.25472
15	8	70	0.015	16.09222	19.60755
16	2	80	0.015	6.058452	12.75687
17	5	80	0.015	11.3256	13.62175
18	8	80	0.015	17.18885	20.07363
19	2	60	0.02	6.022588	6.321959
20	5	60	0.02	10.75737	12.02162
21	8	60	0.02	16.07944	17.4281
22	2	70	0.02	6.269267	6.684978
23	5	70	0.02	11.22636	12.75816
24	8	70	0.02	17.02201	20.41306
25	2	80	0.02	6.793997	13.80338
26	5	80	0.02	12.94095	16.26558
27	8	80	0.02	18.11733	20.63152

**Table 5**  
Analysis of variance for Nu (coded units): a–pure water, b–TiO<sub>2</sub>-W, and c–SiO<sub>2</sub>-W.

a–S = 0.984321						
R-Sq = 96.36%						
R-Sq (adj) = 94.18%						
Source	DF	Seq SS	Adj. SS	Adj. MS	F	P
Main effects	2	127.296	127.296	63.648	65.69	0.000
Q	1	122.419	122.419	122.419	126.35	0.000
T	1	4.877	4.877	4.877	5.03	0.075
2-Way interactions	1	1.024	1.024	1.024	1.06	0.351
Q * T	1	1.024	1.024	1.024	1.06	0.351
Residual error	5	4.844	4.844	0.969		

b–S = 0.332758						
R-Sq = 99.56%						
R-Sq (adj) = 99.40%						
Source	DF	Seq SS	Adj. SS	Adj. MS	F	P
Main effects	3	475.748	475.748	158.583	1432.19	0.000
Q	1	456.947	456.947	456.947	4126.76	0.000
T	1	8.040	8.040	8.040	72.61	0.000
φ	1	10.762	10.762	10.762	97.19	0.000
2-Way interactions	3	3.547	3.547	1.182	10.68	0.000
Q * T	1	1.594	1.594	1.594	14.40	0.001
Q * Fai	1	1.745	1.745	1.745	15.76	0.001
T * Fai	1	0.207	0.207	0.207	1.87	0.187
3-Way interactions	1	0.025	0.025	0.025	0.22	0.643
Q * T * Fai	1	0.025	0.025	0.025	0.22	0.643
Residual error	19	2.104	2.104	0.111		
Total	26	481.423				

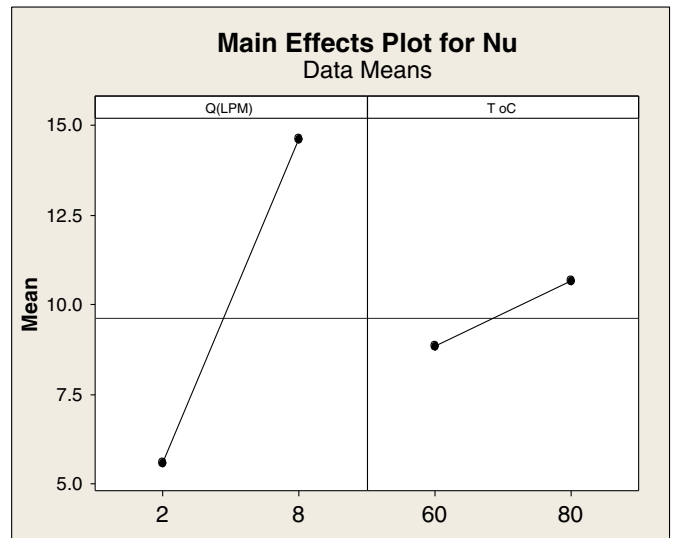
  

c–S = 1.57693						
R-Sq = 92.76%						
R-Sq (adj) = 90.10%						
Source	DF	Seq SS	Adj. SS	Adj. MS	F	P
Main effects	3	598.326	598.326	199.442	80.20	0.000
Q	1	480.631	480.631	480.631	193.28	0.000
T	1	106.347	106.347	106.347	42.77	0.000
φ	1	11.348	11.348	11.348	4.56	0.046
2-Way interactions	3	4.462	4.462	1.487	0.624	0.624
Q(LPM) = * T	1	3.964	3.964	3.964	1.59	0.222
Q * Fai	1	0.176	0.176	0.176	0.07	0.793
T * Fai	1	0.323	0.323	0.323	0.13	0.723
3-Way interactions	1	2.963	2.963	2.963	1.19	0.289
Q * T * Fai	1	2.963	2.963	2.963	1.19	0.289
Residual error	19	47.247	47.247	2.487		
Total	26	652.998				

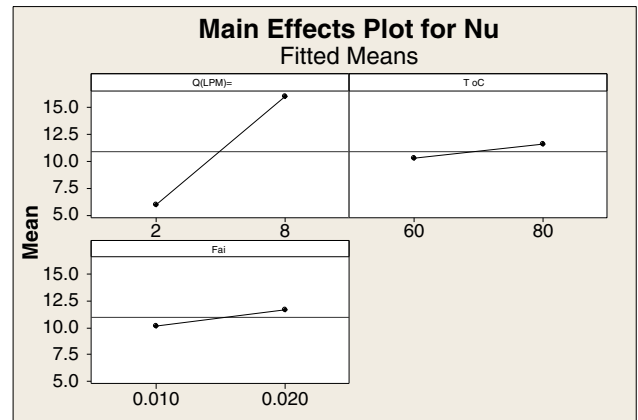
increasing function of Nu; the inlet temperature is almost a linear increasing function of Nu. The volume concentration showed slightly increasing Nu for both nanofluids. The three-dimensional surface plots of Nu with different volume flow rate, inlet temperature and volume concentration values are demonstrated in Fig. 5 for pure water, TiO<sub>2</sub>-W and SiO<sub>2</sub>-W, respectively. The deviations among the measured and predicted responses are illustrated in Fig. 6. The results of the comparison enabled us to predict values of Nu close to those readings recorded experimentally with a confidence of 92–96%.

**Table 6**  
Estimated coefficients for Nu using data in uncoded units.

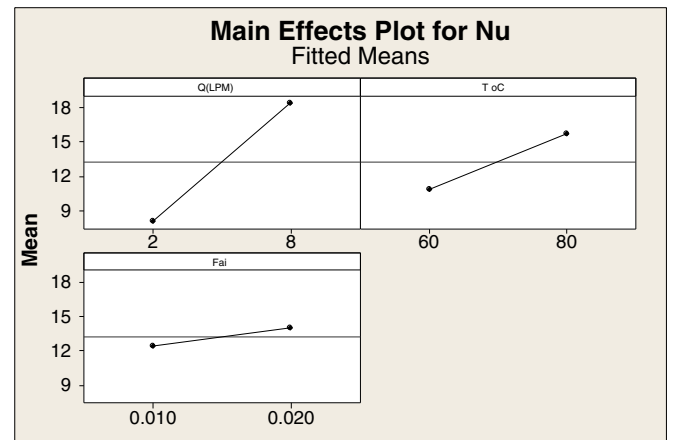
Term	Pure water	TiO <sub>2</sub> -W	SiO <sub>2</sub> -W
Constant	1.69414	6.38776	-3.0125
Q	0.32529	0.060180	-1.31736
T	0.0058446	-0.0610291	0.083777
φ		-285.668	-1071.89
Q * T		0.0176852	
Q * φ		51.2556	



a



b



c

Fig. 4. Main effect plot for Nu: a–pure water, b–TiO<sub>2</sub>-W, and c–SiO<sub>2</sub>-W.

**4. Conclusions**

The forced convection heat transfer enhancement by TiO<sub>2</sub> and SiO<sub>2</sub> suspended in water as a base fluid inside the flat copper tubes of an automotive cooling system has been measured. Significant heat

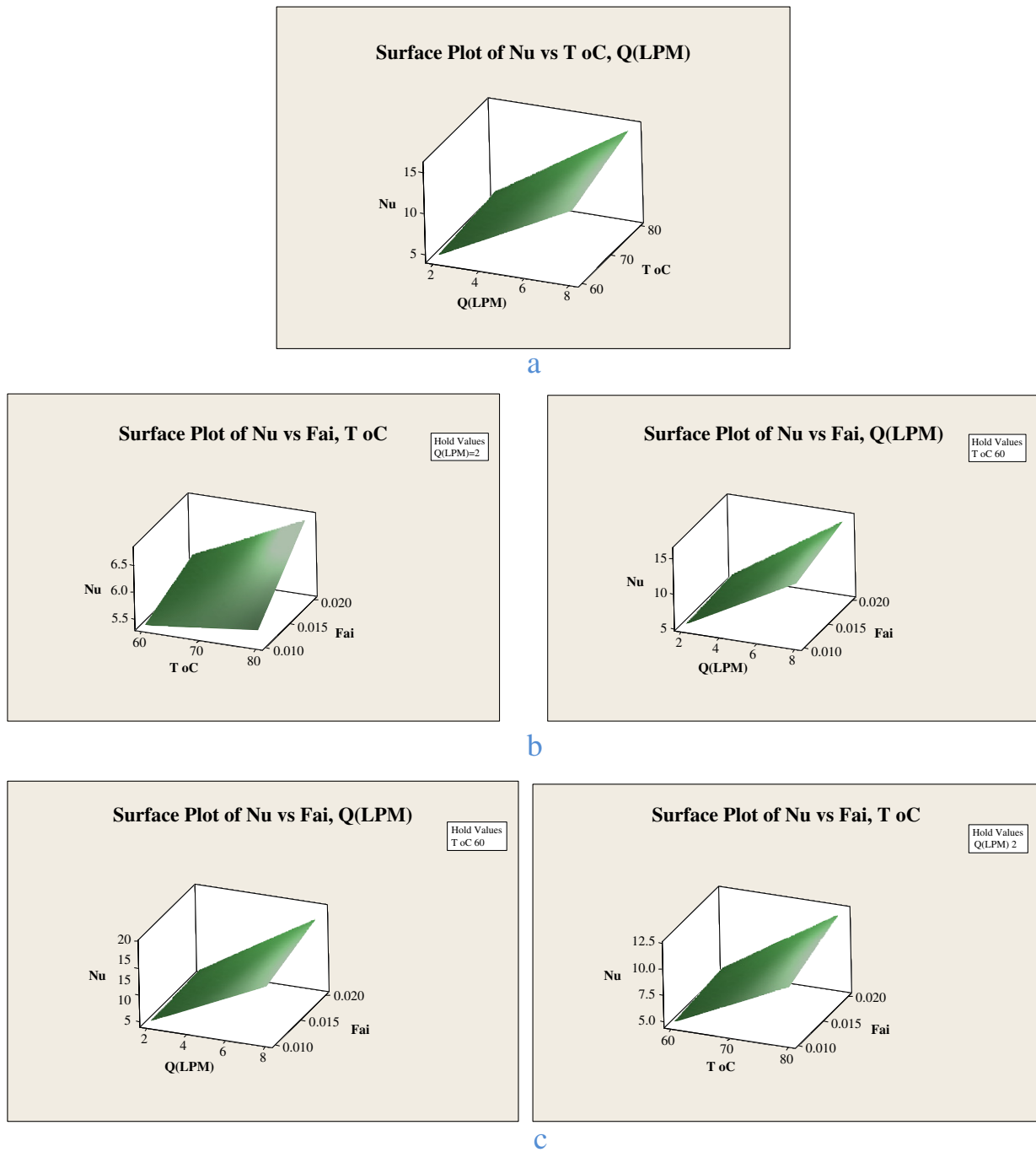


Fig. 5. Surface plot for Nu: a—pure water, b—TiO<sub>2</sub>-W, and c—SiO<sub>2</sub>-W.

transfer enhancement was observed and was associated with the concentration of the nanoparticles. Maximum Nusselt number enhancements of up to 11% and 22.5% were obtained for TiO<sub>2</sub> and SiO<sub>2</sub> nanoparticles, respectively, in water. The experimental results showed that the Nusselt number behaviors of the nanofluids highly depended on the volume flow rate, inlet temperature and nanofluid volume concentration. The results showed that the SiO<sub>2</sub> nanofluid produces a higher heat transfer enhancement than the TiO<sub>2</sub> nanofluid; likewise, TiO<sub>2</sub> nanofluid enhanced heat transfer more than pure water. The results also proved that TiO<sub>2</sub> and SiO<sub>2</sub> nanofluid have a high potential for heat transfer enhancement and are highly appropriate for industrial and practical applications. The input and output

parameters have been tabulated to develop statistical models of cooling system components. These models have been obtained from statistical software using multiple linear regression methods and factorial methodology (FM). The statistical models deduced defined the degree of influence of the volume flow rate, inlet temperature and volume concentration on the Nusselt number. Significant heat transfer augmentation of the cooling system may be achieved by using the highest values of parameters that produce high values of the Nusselt number. The observed heat-transfer enhancements using TiO<sub>2</sub>-W and SiO<sub>2</sub>-W in the cooling system were in good agreement with the experimental data reported by [24,25] and correlate with that of [22] with a deviation of approximately 2–4%.

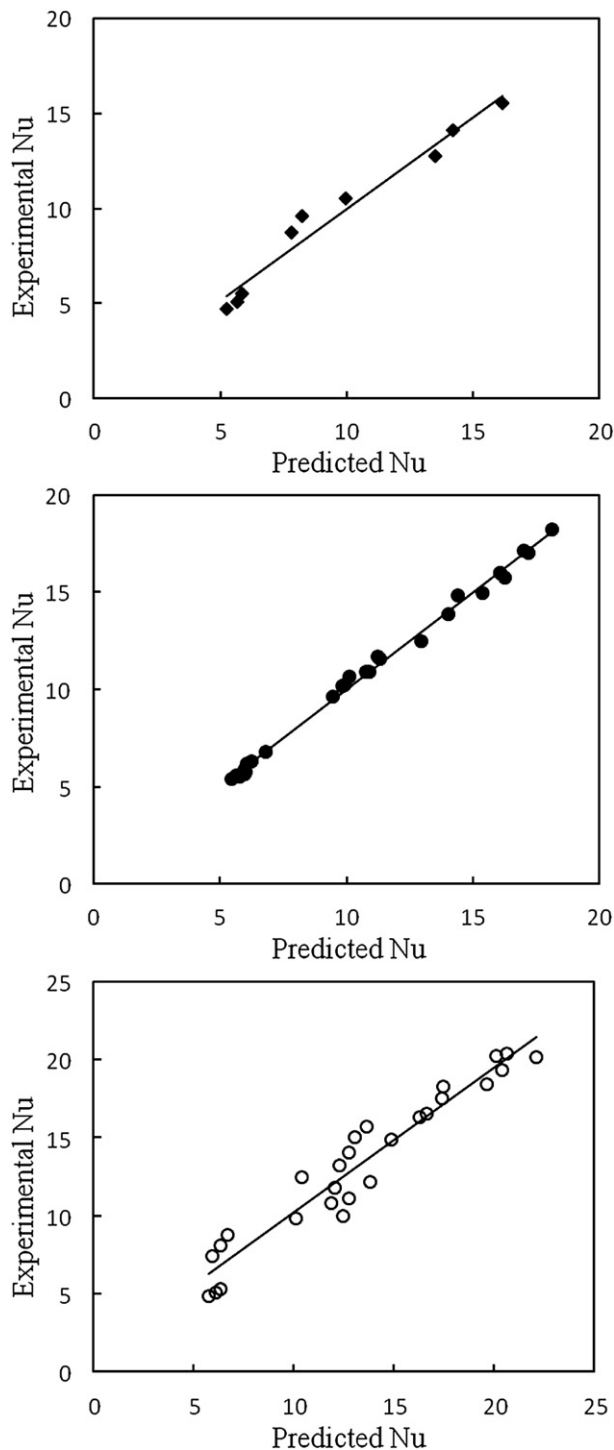


Fig. 6. Comparison of experimental and predicted Nu: a—pure water, b—TiO<sub>2</sub>-W, and c—SiO<sub>2</sub>-W.

### Acknowledgments

The financial support provided to the authors by University Malaysia Pahang is gratefully acknowledged.

### References

- [1] Adnan M. Hussein, K.V. Sharma, R.A. Bakar, K. Kadrigama, A review of forced convection heat transfer enhancement and hydrodynamic characteristics of a nanofluid, *Renew. Sust. Energ. Rev.* 29 (2014) 734–743.
- [2] N. Bozorgan, Evaluation of using Al<sub>2</sub>O<sub>3</sub>-EG and TiO<sub>2</sub>-EG nanofluids as coolants in the double-tube heat exchanger, *Int. J. Adv. Des. Manuf. Technol.* 5 (2012) 27–34.
- [3] W. Duangthongsuk, S. Wongwises, A dispersion model for predicting the heat transfer performance of TiO<sub>2</sub>-water nanofluids under a laminar flow regime, *Int. J. Heat Mass Transf.* 55 (2012) 3138–3146.
- [4] M.E. Meibodi, An estimation for velocity and temperature profiles of nanofluids in fully developed turbulent flow conditions, *Int. Commun. Heat Mass Transf.* 37 (2010) 895–900.
- [5] K. Wongcharee, Enhancement of heat transfer using CuO-water nanofluid and twisted tape with alternate axis, *Int. Commun. Heat Mass Transf.* 38 (2011) 742–748.
- [6] C. Oliet, A. Oliva, J. Castro, C.D.P. Segarra, Parametric studies on automotive radiators, *Appl. Therm. Eng.* 27 (2007) 2033–2043.
- [7] P. Gunnasegaran, N.H. Shuaib, M.F. Abdul Jalal, E. Sandhita, Numerical study of fluid dynamic and heat transfer in a compact heat exchanger using nanofluids, *Int. Sch. Res. Netw. ISRN Mech. Eng.* 2012 (2012) 1–11.
- [8] K.V. Wong, O.D. Leon, Applications of nanofluids: current and future, *Adv. Mech. Eng.* (2010) 1–11.
- [9] R. Saidur, K.Y. Leong, H.A. Mohammad, A review on applications and challenges of nanofluids, *Renew. Sust. Energ. Rev.* 15 (2011) 1646–1668.
- [10] J. Finn, D.J. Ewing, L. Ma, J. Wagner, Nanofluid augmented coolant rail thermoelectric cooling of electronic systems—modeling and analysis, American Control Conference on O'Farrell Street, San Francisco, CA, USA, 2011.
- [11] C. Oliet, C.D. Perezsegarra, A. Oliva, Thermal and fluid dynamic simulation of automotive fin-and-tube heat exchangers, *Heat Transf. Eng.* 29 (5) (2008) 495–502.
- [12] S.M. Peyghambarzadeh, S.H. Hashemabadi, S.M. Hoseini, M. Seifjamani, Experimental study of heat transfer enhancement using water/ethylene glycol based nanofluids as a new coolant for car radiators, *Int. Commun. Heat Mass Transf.* 38 (2011) 1283–1290.
- [13] R.S. Vajjha, D.K. Das, P.K. Namburu, Numerical study of fluid dynamic and heat transfer performance of Al<sub>2</sub>O<sub>3</sub> and CuO nanofluids in the flat tubes of a radiator, *Int. J. Heat Fluid Flow* 31 (2010) 613–621.
- [14] P.K. Trivedi, N.B. Vasava, Study of the effect of mass flow rate of air on heat transfer rate in automobile radiator by CFD simulation using CFX, *Int. J. Eng. Res. Technol.* 1 (6) (2012) 1–4.
- [15] K.W. Park, H.K. Pak, Flow and heat transfer characteristics in flat tubes of a radiator, *Numer. Heat Transf.* 41 (2002) 19–40.
- [16] M. Dehghandokht, M.G. Khan, A. Fartaj, S. Sanaye, Flow and heat transfer characteristics of water and ethylene glycol-water in a multi-port serpentine meso-channel heat exchanger, *Int. J. Therm. Sci.* 50 (2011) 1615–1627.
- [17] K.Y. Leong, R. Saidur, S.N. Kazi, A.M. Mamun, Performance investigation of an automotive car radiator operated with nanofluid-based coolants (nanofluid as a coolant in a radiator), *Appl. Therm. Eng.* 30 (2010) 2685–2692.
- [18] M. Narakia, S.M. Peyghambarzadeh, S.H. Hashemabadi, Y. Vermahmoudi, Parametric study of overall heat transfer coefficient of CuO/water nanofluids in a car radiator, *Int. J. Therm. Sci.* 66 (2013) 82–90.
- [19] A. Bejan, *Convection heat transfer*, Wiley, New York, 2004.
- [20] Adnan M. Hussein, K.V. Sharma, R.A. Bakar, K. Kadrigama, The effect of cross sectional area of tube on friction factor and heat transfer nanofluid turbulent flow, *Int. Commun. Heat Mass Transf.* 47 (2013) 49–55.
- [21] H.B. Hyder, S. Abdullah, R. Zulkifli, Effect of oxides nanoparticle materials on the pressure loss and heat transfer of nanofluids in circular pipes, *J. Appl. Sci.* 12 (13) (2012) 1396–1401.
- [22] R.S. Vajjha, D.K. Das, D.P. Kulkarni, Development of new correlations for convective heat transfer and friction factor in turbulent regime for nanofluids, *Int. J. Heat Mass Transf.* 53 (2010) 4607–4618.
- [23] D.J. Paulo, L. Figueira, Machinability evaluation in hard turning of cold work tool steel (D2) with ceramic tools using statistical techniques, *J. Mater. Des.* 28 (2007) 1186–1191.
- [24] M.Y. Noordin, V.C. Venkatesh, S. Sharif, S. Elting, A. Abdullah, Application of response surface methodology in describing the performance of coated carbide tools when turning AISI 1045 steel, *J. Mater. Process. Technol.* 145 (2004) 46–58.
- [25] S. Ferroillat, A. Bontemps, O. Poncelet, O. Soriano, J. Gruss, Influence of nanoparticle shape factor on convective heat transfer and energetic performance of water-based SiO<sub>2</sub> and ZnO nanofluids, *Appl. Therm. Eng.* 51 (2013) 839e851.
- [26] D. Sing, R. Venkateswara, A surface roughness prediction model for hard turning process, *Int. J. Adv. Manuf. Technol.* 32 (2007) 1115–1124.
- [27] K. Palanikumar, F. Mata, D.J. Paulo, Analysis of surface roughness parameters in turning of FRP tubes by PCD tool, *J. Mater. Process. Technol.* 204 (2008) 469–474.
- [28] K.T. Chiang, Modelling and analysis of the effects of machining parameters on the performance characteristics in the EDM process of Al<sub>2</sub>O<sub>3</sub>-TiC mixed ceramic, *Int. J. Adv. Manuf. Technol.* 37 (2008) 523–533.
- [29] L.B. Abhang, M. Hameedullah, Chip-tool interface temperature prediction model for turning process, *Int. J. Eng. Sci. Technol.* 2 (4) (2010) 382–393.
- [30] B. Fnides, M.A. Yaltese, T. Mabrouki, J.F. Rigal, Application of response surface methodology for determining cutting force model in turning hardened AISI H11 hot work tool steel, *Indian Acad. Sci.* 36 (2011) 109–123.